$K_4GeP_4Se_{12}$: a case for phase-change nonlinear optical chalcogenide

J. I. Jang,[1,*] S. Park,[1] C. M. Harrison,[1] D. J. Clark,[1] C. D. Morris,[2] I. Chung,[2] and M. G. Kanatzidis[2]

[1]*Department of Physics, Applied Physics and Astronomy, Binghamton University, P.O. Box 6000, Binghamton, New York 13902, USA*

[2]*Department of Chemistry, Northwestern University, 2145 Sheridan Road, Evanston, Illinois 60208, USA*

**Corresponding author: jjoon@binghamton.edu*

Received January 22, 2013; accepted March 13, 2013;
posted March 15, 2013 (Doc. ID 184025); published April 10, 2013

We report on broadband nonlinear optical (NLO) responses from a phase-change chalcogenide compound $K_4GeP_4Se_{12}$. Its glassy phase exhibits unusual second-harmonic generation (SHG) due to the preservation of local crystallographic order. The SHG efficiency of the glassy form can be boosted by more than 2 orders of magnitude by simple heat treatment. Strong SHG and third-harmonic generation from both glassy and crystalline compounds were characterized over a wide wavelength range of 1.2–4.0 μm. Our results imply that $K_4GeP_4Se_{12}$ can be utilized for various NLO applications in the mid-infrared spectrum. © 2013 Optical Society of America

OCIS codes: (160.4330) Nonlinear optical materials; (190.2620) Harmonic generation and mixing; (160.2750) Glass and other amorphous materials.

http://dx.doi.org/10.1364/OL.38.001316

Much interest in current optoelectronic applications has involved finding and fabricating highly efficient nonlinear optical (NLO) materials and structures, which can be widely utilized as the active components for tunable coherent light generation [1] as well as for optical signal amplification and switching [2–4]. This is especially true in the mid-infrared (mid-IR) range, which is important for broadband telecommunications [5], environmental monitoring [6,7], medical diagnosis [8], and biological imaging [9,10]. Owing to high refractive indices and excellent transparency in the mid-IR [11], it has been suggested that some noncentrosymmetric chalcogenide crystals could be utilized for second-order NLO applications in this relatively unexplored range [12–15]. Recently, we have reported numerous high-performance chalcogenide-based NLO materials and characterized their properties based on a wavelength-dependent second-harmonic generation (SHG) method [16]. Glassy chalcogenides are also important for mid-IR optoelectronic applications involving various third-order NLO processes [17,18].

In this Letter, we present strong second- and third-order NLO properties of $K_4GeP_4Se_{12}$, which is a rare example of an NLO chalcogenide having reversible crystal-glass phase-change character [19]. $K_4GeP_4Se_{12}$ crystallizes in the noncentrosymmetric polar orthorhombic space group $Pca2_1$ and it is a molecular salt containing $[GeP_4Se_{12}]^{4-}$ clusters that form a pseudo-one-dimensional structure along the [0 1 0] direction. The compound melts congruently in which the melt-quenched amorphous phase undergoes an exothermic glass to crystal phase transition on heating. The measured bandgap energies are 2.0 and 2.1 eV for the crystalline and glassy phases, respectively. Compared with the Raman spectra recorded from the crystalline compound, no peak broadening occurs for the glassy compound, indicating that the $[GeP_4Se_{12}]^{4-}$ molecular anion remains intact even in the glassy phase. This essentially leads to an innate SHG response with no poling treatment [see Fig. 1(a)]. Synthesis as well as basic crystallographic and optical characterization of high-quality $K_4GeP_4Se_{12}$ material are detailed in [19].

Our broadband NLO study was performed on both glassy and crystalline $K_4GeP_4Se_{12}$ powders prepared into eight different particle sizes (d), ranging 20–150 μm. The fundamental beam covering an exceptionally wide mid-IR range ($\lambda = 1.2$–4.0 μm) was produced from an optical parametric oscillator, which was synchronously pumped by an Nd:YAG laser with a pulse width of 30 ps and a repetition rate of 50 Hz. The corresponding energy was tuned to 20 μJ before being focused onto samples with a spot size of 0.5 mm in diameter by a convex lens or a concave gold mirror. However, the data at $\lambda = 2.2$ μm were omitted because the pulse energy was too low. The NLO signals from the samples were collected by a fiber-optic bundle, which was coupled to a selective-grating spectrometer equipped with a CCD camera (detection range: 0.6–1.1 μm) as well as an extended

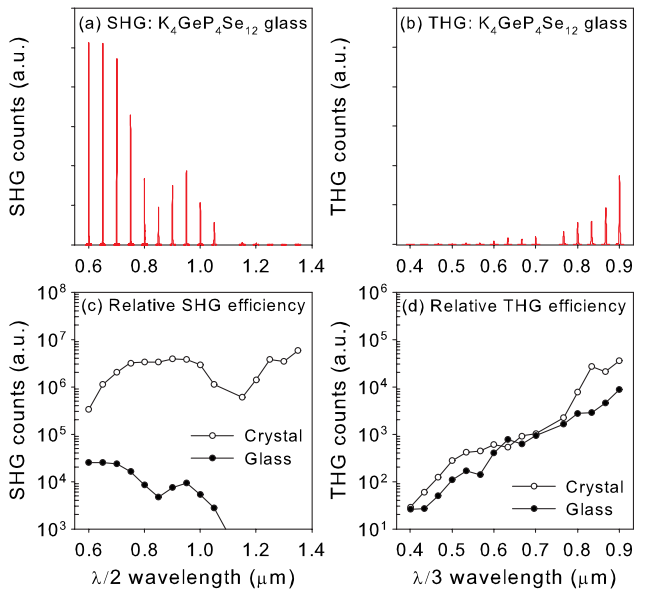

Fig. 1. (a) SHG and (b) THG counts from glassy $K_4GeP_4Se_{12}$ for $\lambda = 1.2$–2.7 μm. Relative SHG and THG counts from glassy (dots) and crystalline (circles) compounds are plotted in parts (c) and (d).

InGaAs detector (detection range: 1.1–2.0 μm). We confirmed that any surface-induced effect as well as NLO signals from other optical components were negligible. The relative NLO signals recorded over a broad wavelength range were precisely calibrated with the known and measured efficiencies of all optical components.

Figure 1(a) plots the observed SHG counts from the glassy $K_4GeP_4Se_{12}$ powders ($d = 53$–63 μm) when λ was varied from 1.2 to 2.7 μm at increments of 0.1 μm. Although the relative SHG efficiency is about 2 orders of magnitude lower than that of the crystalline compound, the glassy phase exhibits significant SHG response [see Fig. 1(c)]. This innate SHG presumably arises because the noncentrosymmetric molecular building blocks remain partially aligned in the amorphous phase. However, the SHG efficiencies for $\lambda/2 > 1.1$ μm are strongly suppressed since the short-range order present in the glassy phase becomes averaged out for longer wavelengths, which in turn cancels out the SHG dipole moments. To our knowledge, only a few glassy chalcogenide compounds, such as $APSe_6$ and $A_2P_2Se_6$ (A = K, Rb) possess such a unique NLO property [20–22].

Figure 1(b) shows third-harmonic generation (THG) from glassy $K_4GeP_4Se_{12}$ under the same experimental conditions. Note that the measured THG counts plummet for $\lambda/3 < 0.59$ μm ($3\omega > 2.1$ eV) due to strong bandgap absorption. Also, THG is more efficient than the lower-order SHG process for $\lambda > 2.2$ μm. Figure 1(d) compares the THG response from the glassy compound (dots) with that from the crystalline compound (circles), indicating that the latter yields several times higher THG efficiencies in our observation range. This is in a sharp contrast to SHG [Fig. 1(c)], eliminating the case of frequency tripling arising from a cascade of SHG and sum-frequency generation ($3\omega = 2\omega + \omega$). Our results imply that the phase-change $K_4GeP_4Se_{12}$ compound is a promising candidate for NLO applications since the glassy compound can be cost-effectively prepared and its NLO efficiencies can be highly enhanced by converting to the crystalline phase with minimal heat treatment.

We now present broadband mid-IR SHG and THG responses up to $\lambda = 4.0$ μm from crystalline $K_4GeP_4Se_{12}$ in comparison with a benchmark IR NLO material $AgGaSe_2$, which was prepared by a similar synthesis method with the same particle sizes. The corresponding SHG and THG wavelength ranges are $\lambda/2 = 0.6$–2.0 μm and $\lambda/3 = 0.4$–1.33 μm, respectively. The series of blue traces in Fig. 2(a) show the measured SHG signals from crystalline $K_4GeP_4Se_{12}$ when we varied λ at increments of 0.1 μm in our experimental range. The red traces correspond to the SHG signals from $AgGaSe_2$ under the same conditions. The sharp decrease in the SHG response occurs when $\lambda/2$ approaches the bandgaps of $K_4GeP_4Se_{12}$ (0.62 μm) and $AgGaSe_2$ (0.72 μm), as indicated by the arrows. This arises due to strong absorption of the produced SHG light near the bandgap as well as two-photon absorption (TPA) of the fundamental beam (see Fig. 3). Similarly, the decrease in the SHG counts in the range of $\lambda/2 = 1.0$–1.2 μm can be attributed to higher-order multiphoton absorption effects. The SHG counts for $\lambda/2 > 1.3$ μm seem to approach a static limit [23] within experimental error bars due to a rather high r.m.s. instability of the input pulses in this range. Although $K_4GeP_4Se_{12}$ is a stronger SHG material than $AgGaSe_2$ in the range of $\lambda/2 = 0.6$–0.9 μm, $AgGaSe_2$ outperforms $K_4GeP_4Se_{12}$ for $\lambda/2 > 1.3$ μm. The blue and red traces in Fig. 3(b) correspond to the broadband THG responses of $K_4GeP_4Se_{12}$ and $AgGaSe_2$, respectively. The THG scans (×100 magnified) are rather similar to the SHG cases except that the THG counts steeply increase beyond the multiphoton absorption edge ($\lambda/3 \simeq 0.8$ μm) due to its cubic dependence on the pump intensity I. High dark counts of the InGaAs detector prevented us from measuring THG for $\lambda > 3.3$ μm, but we predict that THG is essentially λ-independent in this range like SHG. In the static limit, therefore, the THG counts are about 100 times lower than the SHG counts.

The particle size dependence of SHG indicates that $K_4GeP_4Se_{12}$ is not phase-matchable within our observation range. In order to estimate the second-order susceptibility $\chi^{(2)}$ of the compound, we employed Kurtz method [24] at $\lambda = 1.8$ μm, in which both $K_4GeP_4Se_{12}$ and $AgGaSe_2$ are not phase-matchable and minimally affected by absorption effects, yielding $\chi^{(2)} \simeq 11.1$ pm/V with a coherence length $l_c \simeq 50$ μm (see [19] for details). Although evaluation of the NLO index n_2 based on THG is not straightforward due to complications arising from non-phase-matching SHG, we estimated $n_2 \simeq (2.5 \pm 1.2) \times 10^{-14}$ cm^2/W by comparing with the n_2 value of $AgGaSe_2$ and assuming similar THG coherence lengths [25]. We plan to precisely determine n_2 using Z-scan on a thin film prepared by exploiting the congruent melting behavior of the compound. Most importantly, our results clearly emphasize that broadband NLO studies are essential for the characterization of new materials since NLO responses vary widely with λ.

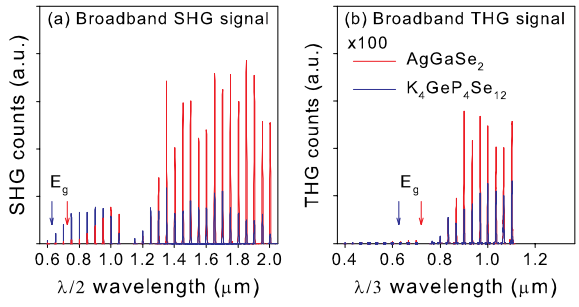

Fig. 2. Broadband (a) SHG and (b) THG responses from $K_4GeP_4Se_{12}$ (blue traces) and $AgGaSe_2$ (red traces). The colored arrows indicate each bandgap.

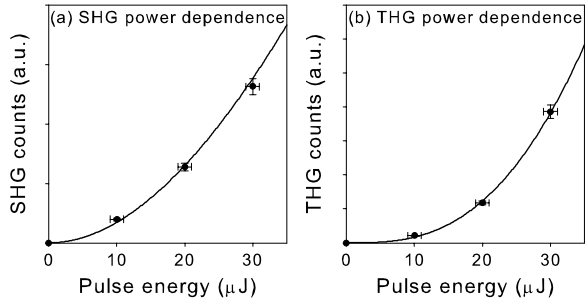

Fig. 3. I dependence of (a) SHG and (b) THG from $K_4GeP_4Se_{12}$ at $\lambda = 1.2$ μm, respectively, superimposed by the TPA fits with $\beta = 30.7$ cm/GW.

We also conducted I-dependent SHG and THG experiments at $\lambda = 1.2$ μm where TPA of the fundamental beam can affect the observed NLO efficiencies of our sample. TPA is a nonparametric NLO process characterized by the TPA coefficient β. The dots in Figs. 3(a) and 3(b) correspond to the measured SHG and THG counts from crystalline $K_4GeP_4Se_{12}$ when the pulse energy was varied from 0–30 μJ. We found that the observed I-dependent SHG and THG cannot be explained by simple I^2 and I^3 fits due to TPA of the pump beam. Assuming slowly varying phase-matching factors, we approximately estimated β by fitting the observed I dependence based on a modified fundamental intensity by TPA:

$$\frac{dI}{dz} = -\beta I^2; \qquad I \to \frac{I}{1+\beta I d}, \tag{1}$$

where $d = 53$–63 μm is the particle size for our reflection-based collection geometry. The curves in Figs. 3(a) and 3(b) correspond to simultaneous fits to the I dependence of SHG and THG with a single fit parameter of $\beta = 30.7 \pm 2.3$ cm/GW, where the uncertainty arises from the uncertainty in d. Except for the multiphoton absorption range, we confirmed that $K_4GeP_4Se_{12}$ has excellent transparency over our observation range, which is an important parameter for NLO applications.

We have investigated broadband mid-IR NLO properties of $K_4GeP_4Se_{12}$ retaining partial noncentrosymmetry even in the amorphous phase and estimated important NLO parameters, such as $\chi^{(2)}$, n_2, and β of the crystalline compound. Owing to the congruent melting behavior of the phase-change compound, NLO devices (for example optical fibers and thin films) [16,20,21] derived from $K_4GeP_4Se_{12}$ can be readily synthesized and the corresponding NLO efficiencies can be significantly improved by minimal heat treatment. By combining apparently unrelated properties of NLO and phase-change behaviors we anticipate a facile approach to creating new NLO materials and devices. The observed strong NLO properties of $K_4GeP_4Se_{12}$ suggest that the compound could be utilized for both second- and third-order NLO applications in the broad range of mid-IR.

This work is supported by the National Science Foundation grant DMR-1104965.

References

1. D. N. Nikogosyan, *Nonlinear Optical Crystals: a Complete Survey*, 1st ed. (Springer, 2005).
2. M. G. Raymer and J. Mostowski, Phys. Rev. A **24**, 1980 (1981).
3. H. M. Gibbs, *Optical Bistability* (Academic, 1985).
4. G. A. Thomas, D. A. Ackerman, P. R. Prucnal, and S. L. Cooper, Phys. Today **53**(9), 30 (2000).
5. D. Cotter, R. J. Manning, K. J. Blow, A. D. Ellis, A. E. Kelly, D. Nesset, I. D. Phillips, A. J. Poustie, and D. C. Rogers, Science **286**, 1523 (1999).
6. M. Pushkarsky, A. Tsekoun, I. G. Dunayevskiy, R. Go, and C. K. N. Patel, Proc. Natl. Acad. Sci. USA **103**, 10846 (2006).
7. M. Pushkarsky, M. E. Webber, T. Macdonald, and C. K. N. Patel, Appl. Phys. Lett. **88**, 044103 (2006).
8. V. A. Serebryakov, E. V. Boiko, N. N. Petrishchev, and A. V. Yan, J. Opt. Technol. **77**, 6 (2010).
9. W. R. Zipfel, R. M. Williams, and W. W. Webb, Nat. Biotechnol. **21**, 1369 (2003).
10. D. Pestov, X. Wang, G. O. Ariunbold, R. K. Murawski, V. A. Sautenkov, A. Dogariu, A. V. Sokolov, and M. O. Scully, Proc. Natl. Acad. Sci. USA **105**, 422 (2008).
11. A. B. Seddon, J. Non-Cryst. Solids **184**, 44 (1995).
12. G. C. Bhar, S. Das, U. Chatterjee, P. K. Datta, and Y. N. Andreev, Appl. Phys. Lett. **63**, 1316 (1993).
13. K. Kato, Appl. Opt. **36**, 2506 (1997).
14. W. Shi, Y. J. Ding, X. Mu, and N. Fernelius, Appl. Phys. Lett. **80**, 3889 (2002).
15. J. H. Liao, G. M. Marking, K. F. Hsu, Y. Matsushita, M. D. Ewbank, R. Borwick, P. Cunningham, M. J. Rosker, and M. G. Kanatzidis, J. Am. Chem. Soc. **125**, 9484 (2003).
16. J. I. Jang, I. Chung, J. B. Ketterson, and M. G. Kanatzidis, in *New Developments in Photon and Materials Research*, J. I. Jang, ed. (NOVA Scientific Publishers).
17. M. Asobe, Opt. Fiber Technol. **3**, 142 (1997).
18. A. Zakery and S. R. Elliott, *Optical Nonlinearities in Chalcogenide Glasses and Their Applications* (Springer, 2007).
19. C. D. Morris, I. Chung, S. Park, C. M. Harrison, D. J. Clark, J. I. Jang, and M. G. Kanatzidis, J. Am. Chem. Soc. **134**, 20733 (2012).
20. I. Chung, J. I. Jang, C. D. Malliakas, J. B. Ketterson, and M. G. Kanatzidis, J. Am. Chem. Soc. **132**, 384 (2010).
21. I. Chung, M.-G. Kim, J. I. Jang, J. He, J. B. Ketterson, and M. G. Kanatzidis, Angew. Chem. Int. Ed. **50**, 10867 (2011).
22. I. Chung, C. D. Malliakas, J. I. Jang, C. G. Canlas, D. P. Weliky, and M. G. Kanatzidis, J. Am. Chem. Soc. **129**, 14996 (2007).
23. J.-H. Song, A. J. Freeman, I. Chung, T. K. Bera, and M. G. Kanatzidis, Phys. Rev. B **79**, 245203 (2009).
24. S. K. Kurtz and T. T. Perry, J. Appl. Phys. **39**, 3798 (1968).
25. http://marzenell.de/Research/Z-Scan/z-scan.html.